Journal of Inflammation Research

Dovepress
open access to scientific and medical research

Open Access Full Text Article

ORIGINAL RESEARCH

MicroRNA-21-3p Engineered Umbilical Cord Stem Cell-Derived Exosomes Inhibit Tendon Adhesion

This article was published in the following Dove Press journal:
Journal of Inflammation Research

Zhixiao Yao[1,*]
Juehong Li[1,*]
Xu Wang[1]
Shiqiao Peng[2]
Jiexin Ning[3]
Yun Qian[1]
Cunyi Fan[1]

[1]Department of Orthopaedics, Shanghai Jiao Tong University Affiliated Sixth People's Hospital, Shanghai 200233, People's Republic of China; [2]Department of Endocrinology, Shanghai Jiao Tong University Affiliated Sixth People's Hospital, Shanghai 200233, People's Republic of China; [3]Department of Plastics, Binzhou People's Hospital, Binzhou 256610, People's Republic of China

*These authors contributed equally to this work

Purpose: As a common complication of tendon injury, tendon adhesion is an unresolved problem in clinical work. The aim of this study was to investigate whether human umbilical cord mesenchymal stem cell-derived exosomes (HUMSC-Exos), one of the most promising new-generation cell-free therapeutic agents, can improve tendon adhesion and explore potential-related mechanisms.

Methods: The rat Achilles tendon injury adhesion model was constructed in vivo, and the localization of HUMSC-Exos was used to evaluate the tendon adhesion. Rat fibroblast cell lines were treated with transforming growth factor β1 (TGF-β1) and/or HUMSC-Exos in vitro, and cell proliferation, apoptosis and gene expression were measured. MicroRNA (miRNA) sequencing and quantitative PCR (qPCR) analysis confirmed differential miRNAs. A specific miRNA antagonist (antagomir-21a-5p) was used to transform HUMSC-Exos and obtain modified exosomes to verify its efficacy and related mechanism of action.

Results: In this study, we found HUMSC-Exos reduced rat fibroblast proliferation and inhibited the expression of fibrosis genes: collagen III (COL III) and α-smooth muscle actin (α-SMA) in vitro. In the rat tendon adhesion model, topical application of HUMSC-Exos contributed to relief of tendon adhesion. Specifically, the fibrosis and inflammation-related genes were simultaneously inhibited by HUMSC-Exos. Further, miRNA sequencing of HUMSCs and HUMSC-Exos showed that miR-21a-3p was expressed at low abundance in HUMSC-Exos. The antagonist targeting miR-21a-3p was recruited for treatment of HUMSCs, and harvested HUMSC-Exos, which expressed low levels of miR-21a-3p, and expanded the inhibition of tendon adhesion in subsequent in vitro experiments.

Conclusion: Our results indicate that HUMSC-Exos may manipulate p65 activity by delivering low-abundance miR-21a-3p, ultimately inhibiting tendon adhesion. The findings may be promising for dealing with tendon adhesion.

Keywords: HUMSC, exosome, tendon adhesion, TGF-β1, p65, miR-21a-3p, NF-κB

Introduction

Tendon damage has a huge economic burden on society. According to incomplete statistics, there are about 3 to 5 million new cases each year.[1] Tendon adhesion is the most common complication of tendon injury. Due to the specificity of tendon healing,[2] tendon adhesion characterized by fibroblast hyperproliferation and extracellular matrix deposition seems to be the inevitable outcome of tendon injury healing.[3] Sliding disorders, loss of function, and reduced mechanical strength constitute major challenges in tendon adhesion. Surgical intervention and rehabilitation programs are

Correspondence: Yun Qian; Cunyi Fan
Department of Orthopaedics, Shanghai Jiao Tong University Affiliated Sixth People's Hospital, Shanghai 200233, People's Republic of China
Tel +86 21-64369181
Email lollipopcloudland@foxmail.com; cyfan@sjtu.edu.cn

submit your manuscript | www.dovepress.com
DovePress
http://doi.org/10.2147/JIR.S254879

dedicated to partially improved outcomes, but there is still room for improvement.[4] In recent years, the development of emerging drugs[5,6] and anti-adhesion biomaterials[7–10] has made up for the shortcomings of the tendon adhesion strategy. However, they all have certain limitations, and the mechanism remains to be elucidated clearly. Revolutionary therapeutic strategies are urgently needed to address this clinically important and intractable challenge.

Exosomes, single-layer (30~200 nm) vesicles, act as communication carriers for DNA, RNA, proteins and lipids. Exosomes and their cargo shuttle between cells for material and signal transmission.[11] With increasing attention, exosomes stand out among numerous therapeutic strategies for their unique advantages.[12] Current areas of application for exosomes include development, immunity, tissue homeostasis, cancer and neurodegenerative diseases.[13] Compared with other exosome donors, human umbilical cord mesenchymal stem cells (HUMSCs) have the advantages of low cost, high efficiency, availability and versatility[14] and are therefore very unique and eye-catching for tissue repair. In particular, compared with MSCs from other tissues, HUMSCs have the same or even higher differentiation potential of cell types related to orthopedic surgical indications.[15–17] In addition, a recent article demonstrated the potential of human umbilical cord blood mesenchymal stem cells to improve chronic full-thickness rotator cuff tearing in a rabbit model.[18] The latest research suggests that exosomes are resistant to fibrosis.[19–21] Exosomes might effectively relieve Crohn's disease and ulcerative colitis by anti-fibrotic and anti-inflammatory effects.[19] Exosomes derived from engineered skin fibroblasts improved skeletal muscle fibrosis in Duchenne mouse muscular dystrophy model.[20] Exosomes loaded with microRNA-19a-3p (miR-19a-3p) improved angiogenesis and reduced myocardial fibrosis in an ischemic heart disease model.[21] Hence, we hypothesize that human umbilical cord mesenchymal stem cell-derived exosomes (HUMSC-Exos) may inhibit tendon adhesion.

MiRNAs, classified as non-coding RNAs,[22] play an important part of the communication function of exosomes. Increasing evidences suggest that microRNA-21 (miR-21) is closely associated with fibrotic disease. Transforming growth factor β (TGF-β), as one of the most active culprits of fibrous diseases, assumes a vital role in the pathological process of tendon adhesion.[23] It was showed that TGF-β transforms quiescent fibroblasts into α-smooth muscle actin (α-SMA)-positive myofibroblasts, which means that the main characterizing cells of tendon adhesion initiate excessive synthesis and secretion extracellular matrix, such as COL III and α-SMA, thereby promoting tendon adhesion.[24] It was reported that miR-21 regulated ERK-MAP kinase signaling in cardiac fibroblasts, thereby regulating cardiac interstitial fibrosis.[25] MiR-21 is one of the most prominent miRNAs in many liver fibrosis models.[26] Inhibition of miR-21 alleviated liver damage, inflammation and fibrosis.[27] MiR-21 was highly elevated in the renal fibrosis model, and interstitial fibrosis was significantly reduced in mice.[28] In addition, our previous research showed that miR-21a-5p was abundant in macrophages, and the low expression of miR-21a-5p macrophage exosomes inhibited tendon adhesion.[29] Similarly, miR-21a-3p, as one member of miR-21 family, was reported to participate in nicotine-stimulated macrophage exosome-induced atherosclerosis,[30] which is clearly inseparable from the course of fibrosis.

In this study, we found HUMSC-Exos inhibited tendon adhesion in vivo and in vitro. Sequencing analysis of miRNA showed the miR-21a-3p content in HUMSC-Exos was of low abundance. We engineered HUMSC-Exos with an antagonist that specifically targeted miR-21 and harvested the low expression of miR-21a-3p HUMSC-Exos to further amplify the effect of inhibiting tendon adhesion. The p65 and Cyclooxygenase-2 (COX2) proteins might be involved in the mediated pathway.

Materials and Methods

Cell Culture and Treatment

HUMSCs used in this study were purchased from the Cell Bank of Chinese Academy of Sciences (Shanghai). The cells were cultured in an α-minimum essential medium (α-MEM, Gibco, Carlsbad, CA, USA) medium mixed with 10% fetal bovine serum (FBS, Gibco, Carlsbad, CA, USA). It was replaced with exosome-depleted-FBS medium when the 3rd-5th passage of HUMSCs reached 50% confluency. The exosome-depleted-FBS was prepared as follows that FBS was ultracentrifuged at 100,000 g for 18 h to predeplete the FBS-derived exosomes[31,32] from FBS-containing medium and obtain FBS-exosome-free, exosome-production medium. After replacing with the exosomes-depleted medium, the cells were cultured for 24–48 hours. The supernatant was collected and the exosomes were collected by ultracentrifugation.

HUMSC cells were cultured in 6-well culture plates. After replacing with the 10% exosome-depleted-FBS medium, cells were transfected with antagonists specifically

targeting has-miR-21a-3p and negative controls (100 nM, RiboBio, Guangzhou, China) using Lipofectamine 3000 (Invitrogen). After 48 hours of culture, the collected supernatant was used to extract engineered HUMSC-Exos ($HUMSC^{antagomir-21}$-Exos/$HUMSC^{antagomir-NC}$-Exos).[30] Rat fibroblast cells (Cell Bank of Chinese Academy of Sciences) were cultured in Dulbecco's Modified Eagle Medium (DMEM) in cell incubator (5% CO^2, 37°C). Cells were collected for subsequent experiments when they were 80% confluent. Fibroblasts were treated with HUMSC-Exos /engineered HUMSC-Exos (100 μg/mL) for 48 h in the presence or absence of TGF-β1 (R&D systems, Minneapolis, MN, USA, 240-B, 2 ng/mL).

Exosomes Isolation

HUMSC cells at 80% confluence were cultured in α-MEM medium with 10% exosome-depleted foetal bovine serum with or without transfection mentioned above for 48 h. Briefly,[33,34] (1) The collected supernatant was centrifuged at 300 g for 10 minutes at 4°C. (2) Retain the supernatant and discard the precipitation. The supernatant was centrifuged at 2000 g for 20 minutes at 4°C. (3) Retain the supernatant and the supernatant was centrifuged at 10,000 g for 30 minutes. (4) The precipitation was discarded, and the collected supernatant was centrifuged at 4°C at 120,000 g for 70 minutes. (5) Resuspend the pellet in PBS and repeat step (4). Finally, the collected exosomes were suspended in PBS to be used directly or frozen at −80°C.

Characterization of Exosomes

Protein quantification of exosomal suspensions was determined using the bicinchoninic acid (BCA) Kit (Beyotime, Beijing, China). Surface markers of exosomes such as anti-CD9, CD63, ALIX and TSG101 (Abcam, Cambridge, MA, USA) were detected by the WB. The morphology and size of exosomes were observed by electron microscopy. Exosomes were fixed at 4°C with 4% paraformaldehyde of equal volume. The exosome suspension was added to the formvar-carbon-coated grids. The exosomes were negatively stained and photographed under an 80 kV electron microscope (Hitachi H7500, Tokyo, Japan). Size distribution and particle concentrations were determined by nanoparticle tracking analysis (NTA; ZetaView PMX 120, Particle Metrix, Meerbusch, Germany).

Animal Experiment

The animal experiment program was approved by the Animal Research Committee of the Sixth People's Hospital affiliated to Shanghai Jiao Tong University. All animal procedures were performed according to the NIH Guide for the Care and Use of Laboratory Animals (No. DWLL2020-0367). The animal strain used in this study was from adult Sprague-Dawley rats, male, weighing about 200~250 g. The rats were housed in ventilated miniature isolation cages with a light and dark cycle of 12 hours, and they were free to eat and move. All rats were anesthetized by intraperitoneal injection of pentobarbital (40 mg/kg). We shaved and disinfected the left hind limb before exposing the Achilles tendon. The superficial Achilles tendon was removed, then cut in the middle of the deep Achilles tendon, and the tendon repair was performed with Kessler suture (6–0 prolene suture, Ethicon, Edinburgh, UK). All the rats were randomly numbered and assigned to the following three experimental groups, sham group, HUMSC-Exos group and PBS group (N=20 per group). The sham group was not treated with other operations. The rats in the HUMSC-Exos group and the PBS group were injected subcutaneously with HUMSC-Exos (200 μg) dissolved in PBS and equal volume of PBS (50 μL). After recovery from anesthesia, all rats were returned to their cages for free movement and weight bearing. Tendon specimens were collected after 3 weeks.

The fresh samples collected were performed for macroscopic evaluation, five independent samples from each group, using the adhesion grading score.[29] 1) no adhesion tissue; 2) adhesion tissue can be separated by blunt dissection; 3) clear and sharp dissection is required, but less than 50% of the adhesion tissue is separated; 4) clear and sharp dissection is required to separate 51 ~ 97.5% of the adherent tissues; 5) clear and sharp dissection is needed, and eventually more than 97.5% of the adherent tissues could be separated.

The collected tendon specimens were made into 5 μm sagittal sections according to standard procedures and stained with H&E and Masson's trichrome. As mentioned previously,[29] five independent samples from each group were used for histological evaluation. Histological adhesion scoring: 1) no adhesion formation; 2) adhesion area is less than 33% of tendon surface; 3) adhesion area accounts for 33–66% of tendon surface; 4) adhesion area exceeds 66% of tendon surface. Histological healing scoring: 1) the tendon has good continuity of the tendon and the surface

of the tendon is smooth; 2) the collagen bundle in the tendon is well repaired, but the epidermis is interrupted by adhesion tissue; 3) the collagen fiber bundle in the tendon is not arranged Regular and partly broken tissues; 4) tendon failed to heal.

The maximum tensile strength was evaluated using a biomechanical analyzer. In short,[29] the tendon specimens were fixed to the Instron 8841 DynaMight axial servo hydraulic test system (Instron, MA, USA) at both ends, and the tendon was stretched at a speed of 30 mm/min until it broke. The experiment was performed with five independent samples from each group.

Immunohistochemically Staining

The tendon sections were immunohistochemically stained according to standard protocols.[25] Samples were processed by following primary antibodies: anti α-smooth muscle actin (α-SMA, Abcam, Cambridge, MA, USA) and anti-collagen III (COL III, Proteintech, Wuhan, China) solution overnight at 4°C. Then, the sections were incubated with the secondary antibody (Cell Signaling Technology) for 30 minutes the next day. For semi-quantitative analysis, the percentage of positively stained cells in six different regions were calculated using Image J software (NIH, Bethesda, MA, USA). With the percentage of cells that stained positive for the antigen in the control group normalized, the relative fold change in other groups was determined.

Cellular Immunofluorescence Staining

As previously described,[35] the differently treated cell slides were fixed with 4% paraformaldehyde for 20 minutes. After blocked, cell slides were incubated with the first antibody (anti-α-SMA and anti-COL III) solution overnight at 4°C in the dark. Next day, the cell slides were incubated with the secondary antibody (Cell Signaling Technology) for 30 minutes. 4′,6-Dimercapto-2-phenylindole (DAPI, Gibco, USA) was used for nuclear staining. Photos were taken by fluorescence microscope (Olympus, FV3000, Japan) and analyzed with Image J software (NIH, Bethesda, MA, USA). The experiment was performed with five independent samples from each group.

MiRNA Sequencing

According to the manufacturer's instructions, total RNA of HUMSC and HUMSC-Exos was extracted using TRIzol reagent (Invitrogen, Carlsbad, CA, USA). The isolated small RNA was end-repaired and reverse transcribed into cDNA to prepare a library. High-resolution (6%) polyacrylamide gel electrophoresis (PAGE, Invitrogen, Carlsbad, CA, USA) was used to separate miRNA libraries with insert sizes ranging from 22 to 24 nt. Quality control and quantification of the constructed sequencing library were carried out. The qualified products were sequenced using the HiSeq™ 2500 platform (Illumina, San Diego, CA, USA) to obtain raw small RNA sequence data. The experiment was performed with three independent samples from each group.

The raw reads were filtered by FASTX-Toolkit software. The quality-controlled reads were BLAST aligned with the miRBase database to obtain a preliminary evaluation of the sequencing results. MiRDeep2 software was used to identify known miRNAs and their expression levels according to the database. Differentially expressed miRNAs (p values < 0.05 and log2/fold change $\neq 0$) were screened using R software package DESeq2. The filtered differentially expressed genes were analyzed by hierarchical clustering and arranged in descending order.

Cell Viability

Cell viability was evaluated using Cell Counting Kit 8 reagents (Dojindo, Kumamoto, Japan) as previously described.[35] Cells were treated with TGF-β1 and/or HUMSC-Exos and then incubated with CCK-8 reagent in 96-well plate for 3h, measured at 450 nm using a microplate reader (SpectraMax® i3x, Molecular Devices, USA). The difference between the optical density (OD) of the test wells and the absorbance of the blank wells represents cell proliferation. The experiment was performed with five independent samples from each group.

Western Blotting

As previously described,[36] tendon tissue or fibroblasts were cleaved by lysate to obtain total protein. The BCA kit was used to determine protein concentration. Total protein was electrophoretically transferred to a PVDF membrane, followed by continuous incubation with primary and secondary antibodies. The primary antibodies used included antiphospho-p65 (p-p65), α-SMA, β-actin (Abeam, Cambridge, MA, USA), and COX2 and Col III (Proteintech, Wuhan, China). Enhanced chemiluminescence solutions (ECL; GE LifeScience, Little Chalfont, Buckinghamshire, UK) and imaging system (Bio-Rad, Hercules, CA, USA) was used for band visualization. Quantification of band intensity from three independent experiments was performed with Image J software, and

the relative protein expression level was normalized to the band intensity of β-actin.

Quantitative PCR (qPCR)

Total RNA was extracted from tendon samples or fibroblasts using TRIzol reagent (Invitrogen, Carlsbad, CA, USA) and RNA was reverse transcribed into cDNA using oligo-dT primer (Takara, Kusatsu, Japan) according to the manufacturer's instructions. Total miRNA Isolation Kit (BioFlux, Japan) was used for total miRNA extraction. Reverse transcription of miRNA into cDNA using TaqMan® MicroRNA Reverse Transcription Kit. Quantitative analysis of gene expression was performed using SYBR Green Premix Ex Taq polymerase (Takara, Kusatsu, Japan). The number of cycles required when the fluorescence signal in each reaction system reaches the set standard is the CT value. The expression level of each sample is represented by $2^{-\Delta\Delta}$ CT. The experiment was performed with five independent samples from each group. GAPDH and U6 were used as standardized internal references for mRNA and miRNA, respectively. Primer sequences were as followed.

α-SMA: Forward 5′-CACCATCGGGAATGAACGCTTC-3′, Reverse 5′-CTGTCAGCAATGCCTGGGTA-3′;

COL III: Forward 5′-AGGTGGGTACACTGTAGCCT-3′, Reverse 5′- GATCGCATAGGTGACAGGTGTT-3′;

GAPDH: Forward 5′-CACTGAGCATCTCCCTCACAA-3′, Reverse 5′- TGGTATTCGAGAGAAGGGAGG-3′;

has-miR-21a-3p: Forward 5′- CTCAACTGGTGTCGTGGAGTCGGCAATTCAGTTGAGACAGCCCA-3′, Reverse 5′-ACACTCCAGCTGGGCAACACCAGTCGATG-3′;

rno-miR-21a-3p: Forward 5′- CTCAACTGGTGTCGTGGAGTCGGCAATTCAGTTGAGGACAGCCC-3′, Reverse 5′-ACACTCCAGCTGGGCAACAGCAGTCGATGG-3′;

U6: Forward 5′-CTCGCTTCGGCAGCACA-3′, reverse 5′-AACGCTTCACGAATTTGCGT-3′.

Dead/Live Staining

We also evaluated cell viability using a dead/live cell stain experiment. Cells were processed using TGF-β1 and/or HUMSC-Exos for 48 h before they were incubated by Dead/Live reagents (Thermo Fisher, USA) for 30 min. Live and dead cells were stained with green and red fluorescence, under the immunofluorescence microscopy (Olympus, FV3000, Japan), respectively. The cell viability was measured by fluorescence using an immunofluorescence microscopy (Olympus, FV3000, Japan). The experiment was performed with five independent samples from each group.

Statistical Analysis

Data are expressed as mean ± the standard deviation (SD). Multiple comparisons were analyzed utilizing one-way analysis of variance (ANOVA). The two groups of comparisons were analyzed utilizing the Student's *t*-test. GraphPad Prism 7 software (GraphPad Prism, USA) was employed for statistical analysis of all data in this study. A P value of less than 0.05 was considered to be statistically significant.

Results

Characterization of HUMSC-Exos

We extracted HUMSC-Exos from the culture medium by gradient ultracentrifugation. As observed by electron microscope, the vesicles were confirmed to be 30–200 nm in diameter (Figure 1). NTA results showed that the average diameter of the collected vesicles was 131 nm (Figure 1). WB was used to detect exosomes' surface markers-CD9, CD63, ALIX and TSG101 were relatively highly positive (Figure 1). The above results indicated that the vesicles we collected were exosomes.

HUMSC-Exos Inhibited Rat Fibroblast Fibrosis in vitro

We used a rat fibroblast cell line as an in vitro model and TGF-β1 as an inducing factor of cell fibrosis. The CCK-8 assay confirmed a proliferative role of TGF-β1 for fibroblasts, but HUMSC-Exos inhibited TGF-β1-induced hyperproliferation (Figure 2). Dead/live staining experiments were employed to assess the relative proportion of dead and living cells, indirectly reflecting cell proliferation. The results showed that TGF-β1 reduced the ratio of dead/live cells ($p < 0.001$). On the contrary, HUMSC-Exos elevated the ratio of dead/live cells ($p < 0.001$)., indicating that HUMSC-Exos inhibited TGF-β1-induced rat fibroblast proliferation (Figure 2). The results of cellular immunofluorescence showed that TGF-β1 induced up-regulation of fibroblast adhesion-related genes COL III and α-SMA, and the addition of HUMSC-Exos significantly inhibited the expression of COL III and α-SMA proteins (Figure 2). We further observed similar conclusions using the WB (Figure 2). The subsequent mRNA analysis data determined by qPCR corroborated this conclusion mentioned above (Figure 2). Collectively, the above data

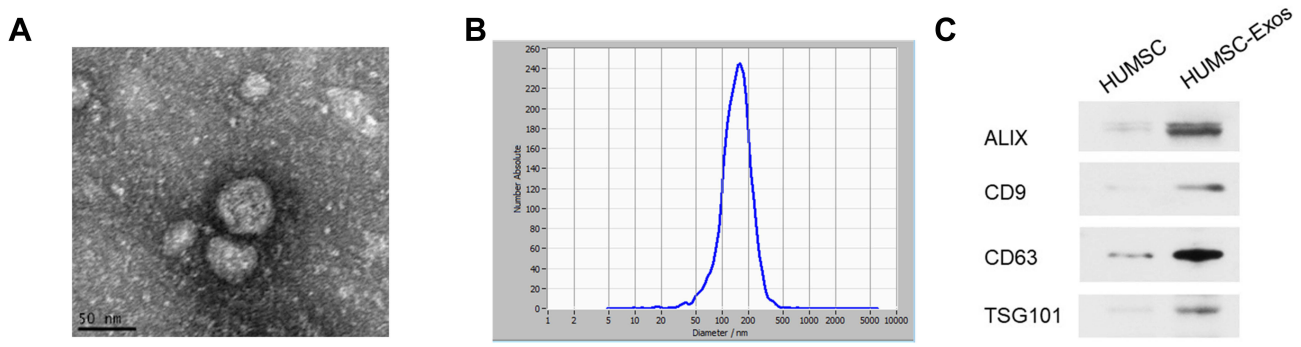

Figure 1 HUMSC-Exos characterization. (**A**) Electron microscope image of collected HUMSC-Exos. (**B**) NTA analysis (n = 3 per group). (**C**) WB images of CD9, CD63, ALIX and TSG101.

indicated that HUMSC-Exos inhibited rat fibroblast proliferation, and simultaneously mitigated fibroblast fibrosis gene expression.

HUMSC-Exos Relieved Tendon Adhesion in Rats

Next, we verified whether HUMSC-Exos could alleviate tendon adhesion in the rat model. After 3 weeks, the rats were euthanized and the tendon specimens were collected for testing. Macroscopic observation showed that the degree of adhesion of tendon tissue with local application of HUMSC-Exos was obviously lighter than that in the PBS group and the sham group (Figure 3). As indicated by the adhesion grade score, the HUMSC-Exos group had the lowest score, and no significant difference was observed between the PBS group and the sham group ($p > 0.05$). H&E staining showed the hyperproliferative adhesion tissue from the HUMSC-Exos group was significantly reduced relative to the sham group, and the degree of inflammatory infiltration was also lower than that of the sham group and the PBS group (Figure 3). Correspondingly, the HUMSC-Exos group had the lowest histological score, which was significantly lower than the sham group ($p < 0.001$) and the PBS group ($p < 0.001$). However, it was worth mentioning that the histological healing score was not statistically different among the three groups ($p > 0.05$). Masson staining showed that the HUMSC-Exos group had the least collagen deposition and was consistent with the H&E staining results (Figure 3).

In particular, in order to assess the effect of HUMSC-Exos on tendon healing, we examined the maximum tensile strength of the three groups of tendons. Consistent with the histological healing scores, no significant differences were detected among the three groups ($p > 0.05$) (Figure 3). These results indicated that local injection of HUMSC-Exos effectively relieved tendon adhesion in rats without side effects of reduced biomechanical performance. To further demonstrate the effect of HUMSC-Exos on tendon adhesion, we performed immunohistochemical staining of tendon specimens. The results indicate that HUMSC-Exos significantly decreased COL III and α-SMA expression ($p < 0.01$ and $p < 0.001$, respectively) (Figure 4). The results of qPCR and WB were similar to this (Figure 4). Furthermore, we used WB to measure the expression of the inflammatory genes p-p65 and COX2, and the data indicated that HUMSC-Exos dramatically suppressed the protein levels of the inflammatory-related genes p-p65 and COX2 in synchronization with the inhibition of COL III and α-SMA expression. The above results indicated that HUMSC-Exos may inhibit rat tendon adhesion by regulating the expression of the inflammatory genes p65 and COX2.

MiRNA Sequencing Showed Low Abundance of miR-21a-3p in HUMSC-Exos

We sequenced the miRNA between HUMSC-Exos and HUMSCs, and miR-21a-3p was listed among the top 20 most differentially expressed miRNAs (Figure 5). Further confirmed by qPCR, the content of has-miR-21a-3p in HUMSC-Exos was significantly lower than that in HUMSCs ($p < 0.001$) (Figure 5). Meanwhile, we examined the content of rno-miR-21a-3p in the tendon specimens of the HUMSC-Exos group and the sham group. The results indicated that after topical application of HUMSC-Exos, the levels of rno-miR-21a-3p in rat tendons decreased ($p < 0.001$) (Figure 5). These results indicated that HUMSC-Exos had low abundance of miR-21a-3p compared with HUMSCs and local application

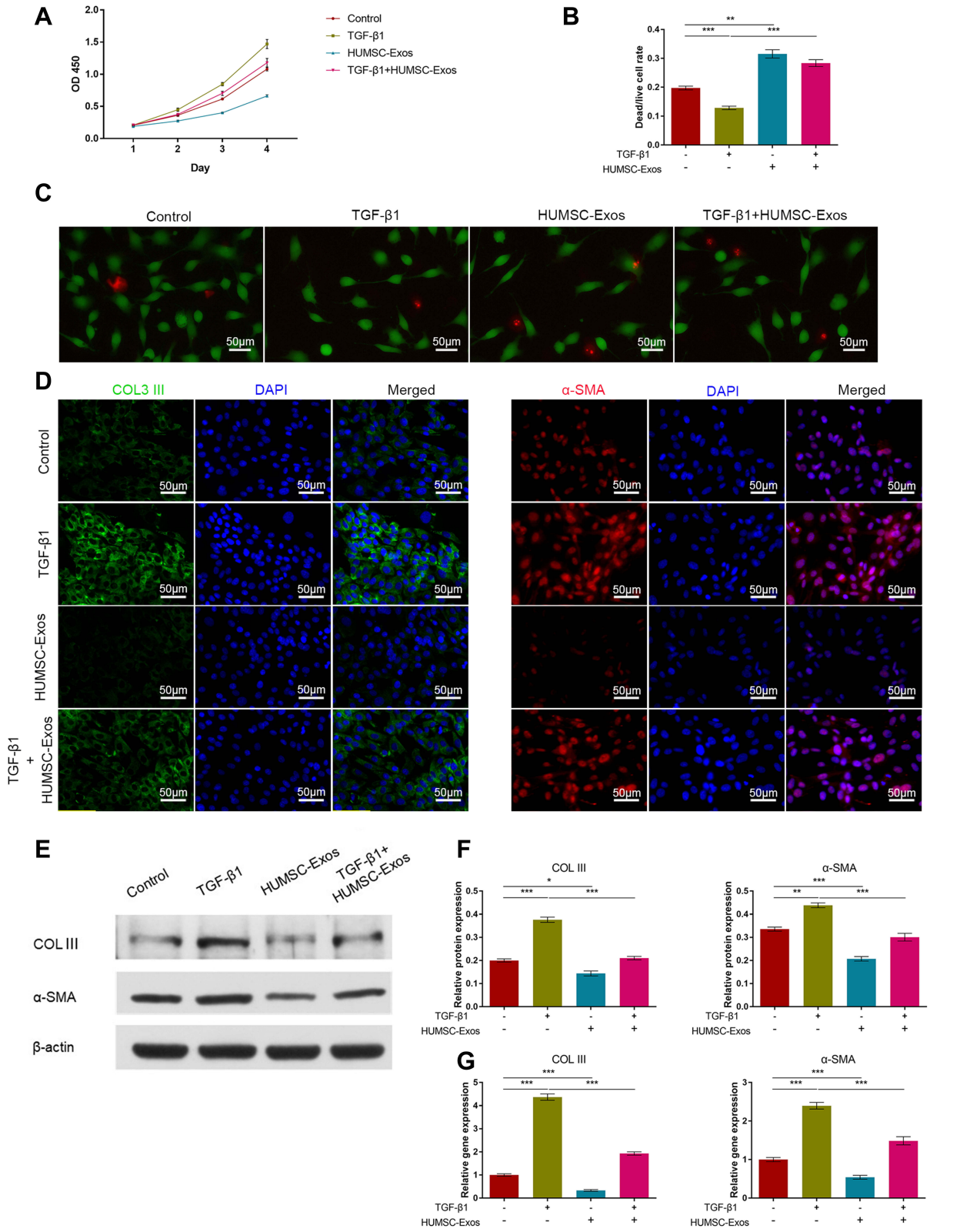

Figure 2 HUMSC-Exos inhibited rat fibroblast proliferation and fibrosis and promoted apoptosis. Rat fibroblasts were treated with HUMSC-Exos in the presence or absence of TGF-β1. (**A**) Cell proliferation (n = 5 per group). (**B**) Dead/live analysis (n = 5 per group). (**C**) Representative images of dead/live cells stained. Scale bar: 50 μm. (**D**) Cellular immunofluorescence images of COL III and α-SMA. Scale bar: 50 μm. (**E**) WB images of COL III and α-SMA. (**F**) Quantification of COL III and α-SMA (n = 3 per group). (**G**) Quantitative analysis of mRNA for COL III and α-SMA (n = 5 per group). *P < 0.05, **P < 0.01, ***P < 0.001.

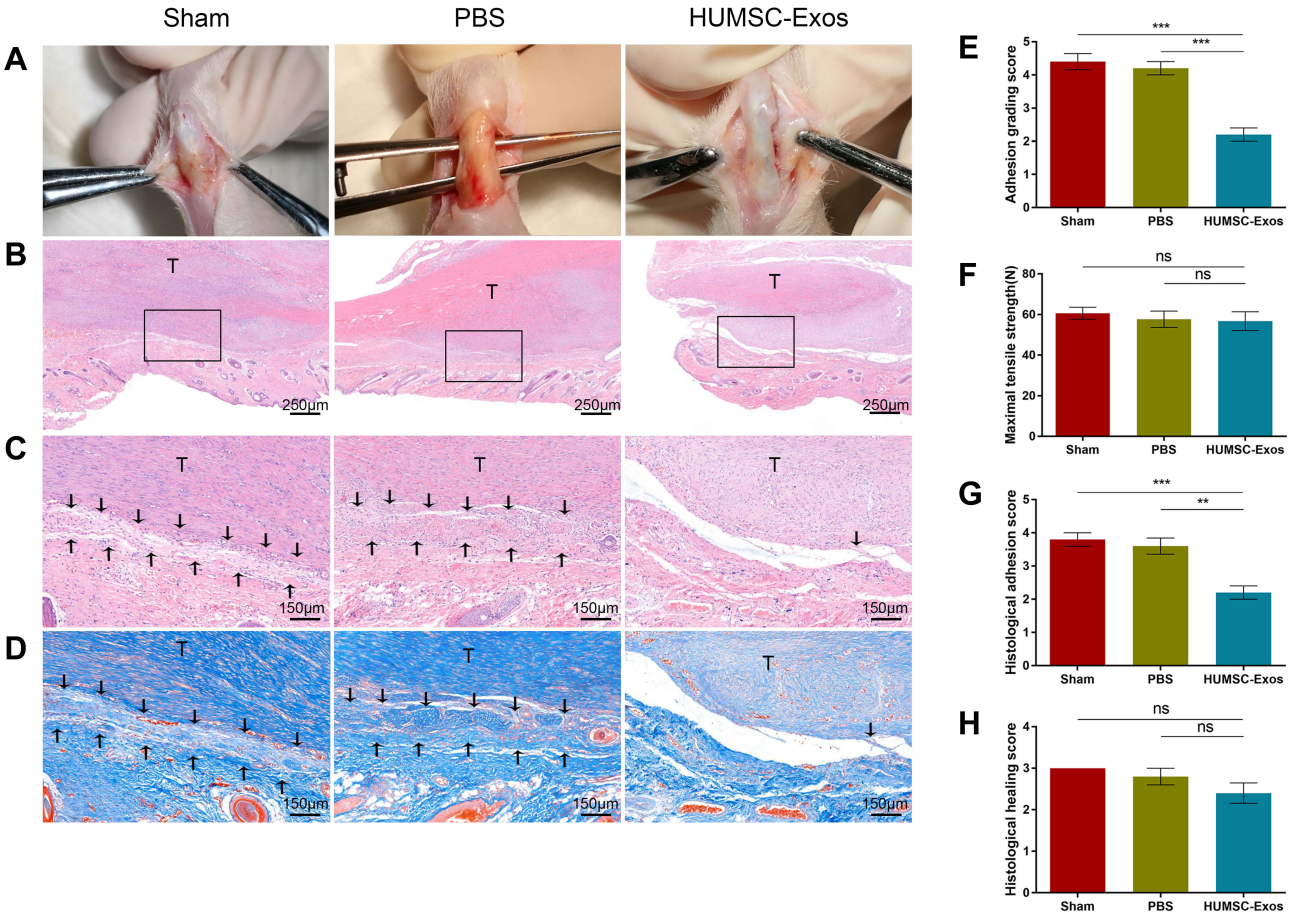

Figure 3 HUMSC-Exos inhibited tendon adhesion in rats. Rat tendon tissue from the sham, PBS and HUMSC-Exos groups was collected 3 weeks after surgery. (**A**) Macroscopic observation of tendons. (**B** and **C**) H&E staining of tendon sections. (**D**) Masson staining of tendon sections. (**E**) Adhesion grading score (n = 5 per group). (**F**) Maximum tensile strength (n = 5 per group). (**G**) Histology adhesion score (n = 5 per group). (**H**) Histological healing score (n = 5 per group). **P < 0.01, ***P < 0.001. (**C** and **D**) The arrows refer to adhesion tissues.
Abbreviation: ns, not significant.

HUMSC-Exos decreased the expression of miR-21a-3p in rat tendon. Next, we pretreated HUMSC with antagonists targeting human miR-21a-3p to obtain modified HUMSC-Exos. qPCR results showed that miR-21a-3p in HUMSC-Exos was significantly decreased ($p < 0.001$) (Figure 5), indicating that we successfully obtained engineered HUMSC-Exos with low expression of has-miR-21a-3p.

Engineered HUMSC-Exos Expanded the Inhibition of Tendon Adhesion

We further validated the effect of engineered HUMSC-Exos on fibroblasts in vitro. The results of WB indicated that HUMSC-Exos, which underexpressed miR-21a-3p, further inhibited the expression of COL III and α-SMA in fibroblasts ($p < 0.01$ and $p < 0.001$, respectively) (Figure 6, in parallel with the inflammation-related genes p-p65 and COX2 ($p < 0.01$ and $p < 0.001$, respectively) (Figure 6). These results indicated that HUSMC-Exos inhibited tendon fibrosis by delivering low abundance of miR-21a-3p to regulate p65 activity. Fortunately, HUMSC-Exos, which was engineered with low expression of miR-21a-3p, further amplified its role in inhibiting fibrosis.

Discussion

In this study, we first found that HUMSC-Exos inhibited tendon adhesion in vivo and in vitro. HUMSC-Exos inhibited the levels of inflammation-related genes p-65 and COX2 in vivo. By comparing the miRNA sequencing data between HUMSCs and HUMSC-Exos, we found that miR-21a-3p was of low abundance in HUMSC-Exos. An antagonist targeting specific miR-21a-3p was employed to engineer HUMSCs, the harvested HUMSC-Exos with low expression miR-21a-3p further inhibited tendon fibrosis progression, and our data indicated that

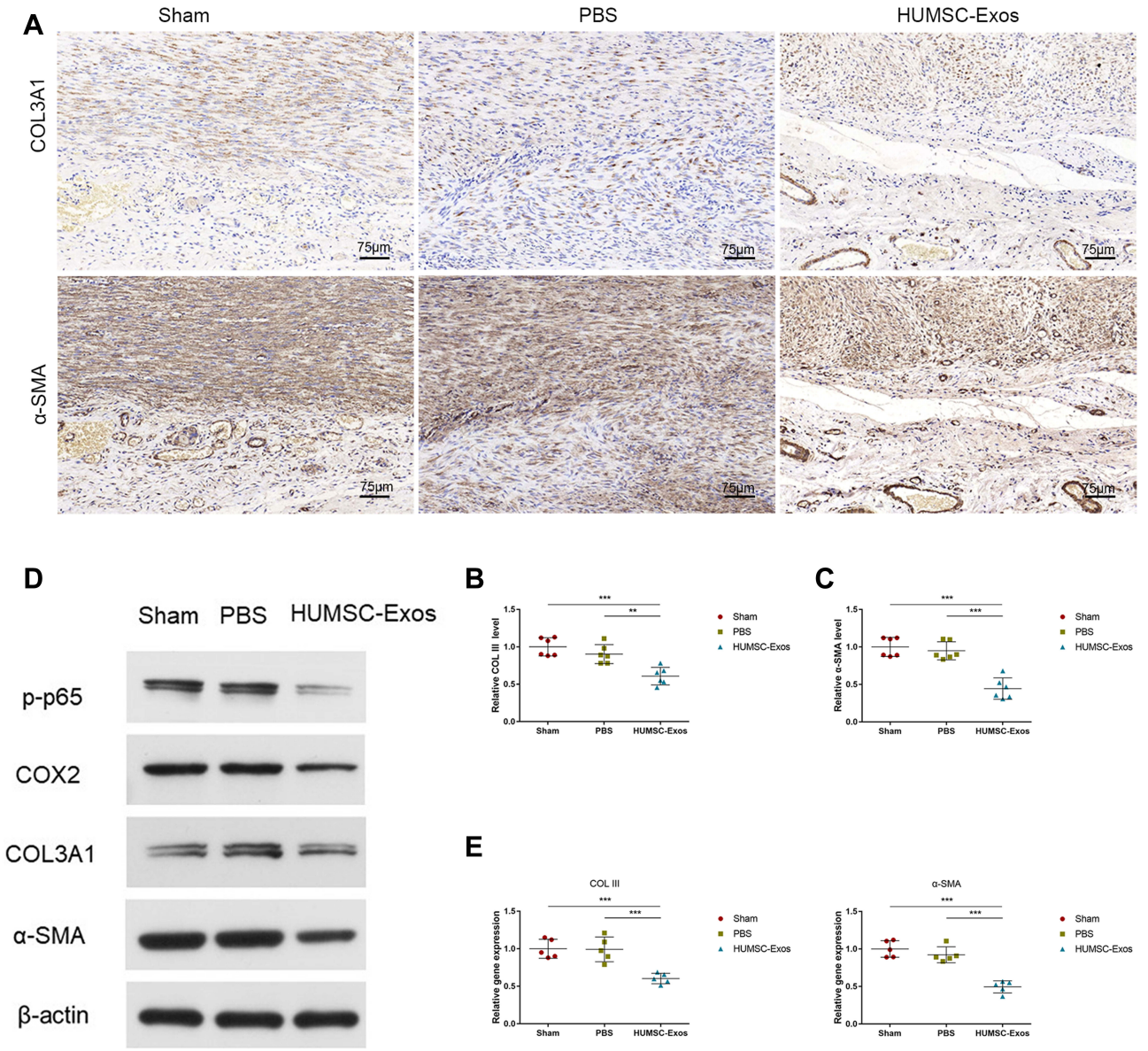

Figure 4 HUMSC-Exos synchronously inhibited rat tendon fibrosis and p65 activity. (**A**) Immunohistochemical staining of COL III and α-SMA. Scale bar: 75 μm. (**B** and **C**) Quantitative analysis of COL III and α-SMA (n = 6 per group). (**D**) WB images of COL III and α-SMA. (**E**) Quantitative analysis of mRNA for COL III and α-SMA (n = 5 per group). **P < 0.01, ***P < 0.001.

HUMSC-Exos inhibited tendon adhesion by delivering low-abundance miR-21a-3p to manipulating p65 activity.

The pathological hallmark of fibrotic diseases is the excessive deposition of extracellular matrix represented by COL III and α-SMA. Endogenous healing after tendon injury is driven by autologous cell proliferation,[37] and exogenous healing based on periorbital and recruitment cells contributes to the overproduction of fibrous adhesion tissue.[38] As a novel generation of cell-free nanomaterial, HUMSC-Exos has demonstrated promising efficacy in many areas of tissue repair. The currently proven role of HUMSC-Exos included accelerated skin,[39] vaginal[40] and fracture healing,[41] reduction of type 2 diabetes.[42] It is not difficult to find that HUMSC-Exos promoted tissue repair often associated with inhibition of excessive proliferation of fibrotic tissue. In our study, we found in the rat tendon adhesion model that local injection of HUMSC-Exos inhibited the expression of fibrosis genes COL III and α-SMA. In vitro, we found that HUMSC-Exos significantly inhibited TGF-β1-inducted fibroblast proliferation, which paralleled to the observed inhibition of COL III and α-SMA expression. These results preliminarily indicated that topical application of HUMSC-Exos contributed to alleviate tendon adhesion. Recently, HUMSC-Exos pretreatment attenuated TGF-β-induced

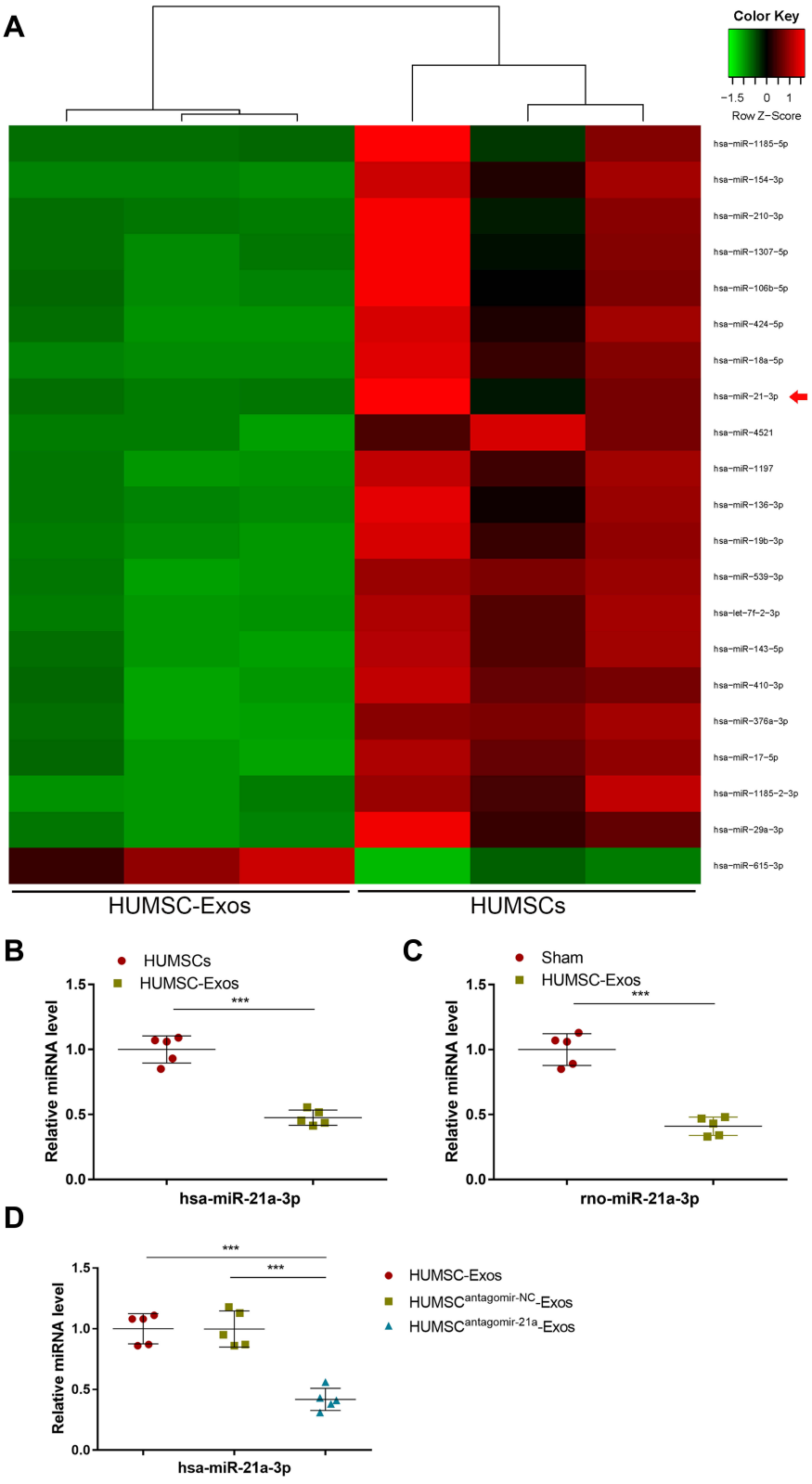

Figure 5 HUMSC-Exos expressed low abundance of miR-21a-3p. (**A**) The top 20 miRNAs with the most significant differences. (**B**) qPCR analysis of has-miR-21a-3p in HUMSCs and HUMSC-Exos (n = 5 per group). (**C**) qPCR analysis of rno-miR-21a-3p in tendon tissues from C HUMSC-Exos and sham groups (n = 5 per group). (**D**) The expression of has-miR-21a-3p determined by qPCR (n = 5 per group). ***P < 0.001.

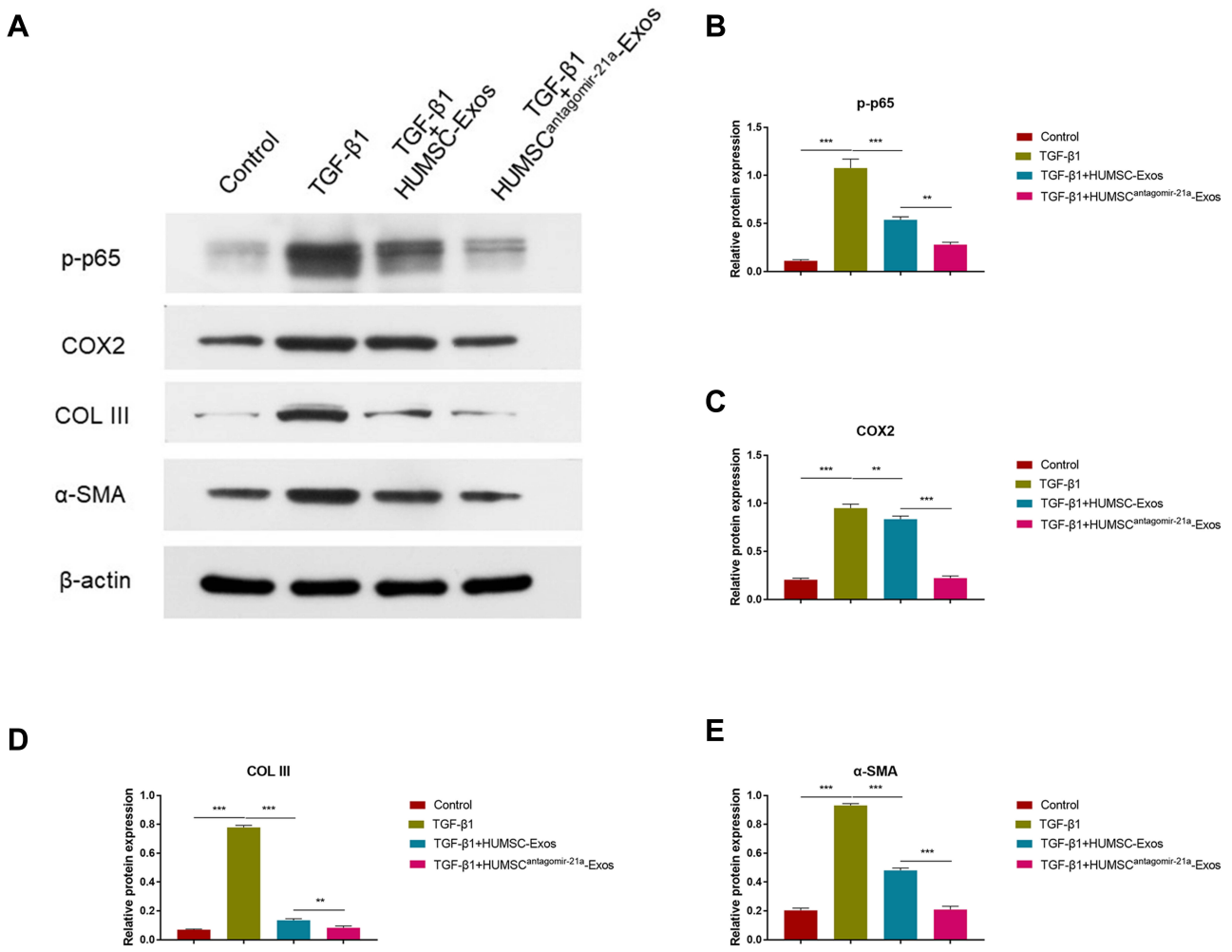

Figure 6 Engineered modification of HUMSC-Exos expanded inhibition of fibrosis. Rat fibroblasts were treated with HUMSC-Exos or HUMSC$^{antagomir-21}$-Exos for 48 h in the presence or absence of TGF-β1. (**A**) WB images of p-p65, COX2, COL III and α-SMA. (**B**–**E**) Quantification of p-p65, COX2, COL III and α-SMA (n = 3 per group). **P < 0.01, ***P < 0.001.

cardiac fibroblast secretion of α-SMA.[43] Intramuscular injection of exosomes/miR-29 partially inhibited renal fibrosis in mice, showing a decrease in α-SMA, fibronectin and collagen I.[44] Our results were consistent with previous studies.

It is well known that nuclear factor (NF)-κB is a classical inflammation-mediated pathway, and the RelA/p65 protein is considered to be a core element in the NF-κB pathway.[45] A large body of evidence confirms the role of p65 in fibrosis. NF-κB activation was closely associated with fibrosis in chronic pancreatitis[46] and fibrosis after liver damage.[47] Myocardial NADPH oxidase 4 (Nox4) caused myocardial fibrosis partially through the NF-κB signaling pathway.[48] Targeting NF-κB helped to alleviate the progression of rheumatoid arthritis.[49] We previously found up-regulated p-p65 and COX2 in human tendon adhesions and mouse tendons and inhibited RelA/p65 contributed to alleviating tendon adhesion in mice.[6] In addition, it was reported that MSC-Exos attenuated lipopolysaccharide (LPS)-induced astrocyte proliferation and inactivated NF-κB signaling.[50] Our results were consistent with this. HUMSC-Exos inhibited tendon adhesion while inhibiting the expression of p-p65 and COX2, indicating that HUMSC-Exos may inhibit tendon adhesion by inhibiting p-p65 and COX2.

Confirmed by detailed evidence, miR-21 is recognized for regulating tissue fibrosis.[25,27,28.] Inhibition of miR-21 helps to alleviate the progression of fibrosis.[25,27] In our previous research, we preliminarily confirmed the important role of macrophage exosomes in the occurrence of tendon adhesion. Mechanistically, high-throughput miRNA sequencing of macrophage exosomes revealed that miR-21-5p was highly enriched. The miR-21 mimic was subsequently used to confirm the hypothesis that miR-21-5p promotes tendon fibrosis by mediating Smad7 expression.[22] This study verified the association between miR-21 and tendon adhesion,

and provided a theoretical basis for improving tendon adhesion by targeting exosome-derived miR-21. In this study, firstly, we proved the novel anti-fibrotic field of HUMSC-Exos, that is, anti-tendon adhesion. Based on this fact, we cautiously suspected that the fibrosis-mediated factor miR-21 in HUMSC-Exos was under-expressed. As predicted, miR-21a-3p was screened of low expression in HUMSC-Exos through the miRNA sequencing between HUMSC and HUMSC-Exos. Surprisingly, HUMSC-Exos had lower miR-21a-3p content than that in HUMSCs, which implied that the pros and cons of anti-fibrosis of the two may be attributed to the different miR-21a-3p content. Then, we treated HUMSCs with an antagonist that specifically targets human miR-21a-3p to obtain HUMSC-Exos with low expression of miR-21a-3p. Subsequent in vitro experiments showed that engineered HUMSC-Exos, which underexpressed miR-21a-3p, further inhibited tendon fibrosis. In addition, the level of suppressed adhesion gene expression coincided with downregulation of p-p65 and COX2. Therefore, we hypothesized that HUMSC-Exos inhibited the p65 activity by low-abundance miR-21-3p and thus relieved tendon adhesion. In fact, some scholars reported that down-regulation of miR-21 inhibited PI3K/Akt-NF-κB signaling pathway and promoted apoptosis in OVCAR3 cells.[51] This was consistent with our study that HUMSC-Exos underexpressed miR-21a-3p, synchronizing with p65 inactivation and inhibited cell viability in fibroblasts. In contrast, some scholars found that after treatment with miR-21 mimic-loaded human peripheral blood-derived exosomes, gene expression levels of mothers against decapentaplegic homolog 3 (Smad7), phosphatase and tension homologue (PTEN) and matrix metalloproteinase 2 (MMP2) associated with cardiac fibrosis increased both in vivo and in vitro. Furthermore, miR-21 mimic-loaded exosomes enhanced fibrosis in the mouse model of myocardial infarction.[52] Similarly, a study of renal fibrosis reported that treatment with miR-21 significantly aggravated the TGF-β-induced epithelial fibroblast phenotype.[53] Thus, overexpression of mir-21 may tend to fibrosis. This study initially achieved the goal of improving the adhesion of tendon by manipulating exosome-derived miR-21.

Collectively, we extended the tissue repair effect of HUMSC-Exos to the field of anti-tendon adhesion, and confirmed that it may be inseparable from the classic fibrosis factor miR-21. This provides a novel treatment strategy for the treatment of tendon fibrosis, especially by manipulating the expression of specific cargoes of exosomes, such as miR-21, to optimize the treatment effect. However, this experiment has the following limitations. Firstly, in vivo studies did not do dose optimization; secondly. Secondly, in vitro studies did not explore the effect of HUMSC-Exos on tenocyte. Lastly, as for the mechanism, especially the relationship between the miR-21 family and the p65 pathway, further systematic studies are needed.

Conclusions

In summary, we innovatively introduced the cell-free therapeutic agent HUMSC-Exos into the field of tendon adhesion. The anti-tendon fibrosis effect of HUMSC-Exos was validated in vitro and in vivo. The differential expression of miR-21a-3p between HUMSC-Exos and HUMSCs determined by miRNA sequencing provided a basis for engineering modification of exosomes. An antagonist targeting miR-21a-3p was recruited to underexpress miR-21a-3p in exosomes, and the harvested modified HUMSC-Exos further expanded the inhibition of tendon adhesion and possibly by manipulation of p65 activity.

Abbreviations

HUMSC(s), human umbilical cord mesenchymal stem cell(s); HUMSC-Exo(s), human umbilical cord mesenchymal stem cell-derived exosome(s); COL III, collagen III; α-SMA, α-smooth muscle actin; TGF-β1, transforming growth factor-β1; NF-κB, nuclear factor-κB; COX2, cyclooxygenase-2; NTA, nanoparticle tracking analysis.

Acknowledgments

The study was supported by the National Natural Science Foundation of China (No. 81830076 and No. 81672146) and the Projects of Science and Technology Development Foundation of Pudong New District, Shanghai, China (Grant No. PWZxq2017-03). We appreciate the support from Youth Science and Technology Innovation Studio of Shanghai Jiao Tong University School of Medicine.

Disclosure

The authors report no conflicts of interest in this work.

References

1. de Jong JP, Nguyen JT, Sonnema AJ, Nguyen EC, Amadio PC, Moran SL. The incidence of acute traumatic tendon injuries in the hand and wrist: a 10-year population-based study. *Clin Orthop Surg*. 2014;6(2):196–202. doi:10.4055/cios.2014.6.2.196
2. Nourissat G, Berenbaum F, Duprez D. Tendon injury: from biology to tendon repair. *Nat Rev Rheumatol*. 2015;11(4):223–233. doi:10.1038/nrrheum.2015.26
3. Morita W, Snelling SJSJB, Dakin SG, Carr AJ. Profibrotic mediators in tendon disease: a systematic review. *Arthritis Res Ther*. 2016;18(1):269. doi:10.1186/s13075-016-1165-0

4. Nichols AEC, Best KT, Loiselle AE. The cellular basis of fibrotic tendon healing: challenges and opportunities. *Transl Res*. 2019;209:156–168. doi:10.1016/j.trsl.2019.02.002
5. Zheng W, Qian Y, Chen S, Ruan H, Fan C. Rapamycin protects against peritendinous fibrosis through activation of autophagy. *Front Pharmacol*. 2018;9:402. doi:10.3389/fphar.2018.00402
6. Chen S, Jiang S, Zheng W, et al. RelA/p65 inhibition prevents tendon adhesion by modulating inflammation, cell proliferation, and apoptosis. *Cell Death Dis*. 2017;8(3):e2710. doi:10.1038/cddis.2017.135
7. Jiang S, Zhao X, Chen S, et al. Down-regulating ERK1/2 and SMAD2/3 phosphorylation by physical barrier of celecoxib-loaded electrospun fibrous membranes prevents tendon adhesions. *Biomaterials*. 2014;35 (37):9920–9929. doi:10.1016/j.biomaterials.2014.08.028
8. Zhou Y, Zhang L, Zhao W, Wu Y, Zhu C, Yang Y. Nanoparticle-mediated delivery of TGF-beta1 miRNA plasmid for preventing flexor tendon adhesion formation. *Biomaterials*. 2013;34(33):8269–8278. doi:10.1016/j.biomaterials.2013.07.072
9. Shalumon KT, Sheu C, Chen CH, et al. Multi-functional electrospun antibacterial core-shell nanofibrous membranes for prolonged prevention of post-surgical tendon adhesion and inflammation. *Acta Biomater*. 2018;72:121–136. doi:10.1016/j.actbio.2018.03.044
10. Zhou YL, Yang QQ, Yan YY, Zhu C, Zhang L, Tang JB. Localized delivery of miRNAs targets cyclooxygenases and reduces flexor tendon adhesions. *Acta Biomater*. 2018;70:237–248. doi:10.1016/j.actbio.2018.01.047
11. Pluchino S, Smith JA. Explicating exosomes: reclassifying the rising stars of intercellular communication. *Cell*. 2019;177(2):225–227. doi:10.1016/j.cell.2019.03.020
12. Colao IL, Corteling R, Bracewell D, Wall I. Manufacturing exosomes: a promising therapeutic platform. *Trends Mol Med*. 2018;24 (3):242–256. doi:10.1016/j.molmed.2018.01.006
13. Pegtel DM, Gould SJ. Exosomes. *Annu Rev Biochem*. 2019;88 (1):487–514. doi:10.1146/annurev-biochem-013118-111902
14. Capelli C, Gotti E, Morigi M, et al. Minimally manipulated whole human umbilical cord is a rich source of clinical-grade human mesenchymal stromal cells expanded in human platelet lysate. *Cytotherapy*. 2011;13(7):786–801. doi:10.3109/14653249.2011.563294
15. Baksh D, Yao R, Tuan RS. Comparison of proliferative and multilineage differentiation potential of human mesenchymal stem cells derived from umbilical cord and bone marrow. *Stem Cells*. 2007;25 (6):1384–1392. doi:10.1634/stemcells.2006-0709
16. De la Fuente A, Mateos J, Lesende-Rodríguez I, et al. Proteome analysis during chondrocyte differentiation in a new chondrogenesis model using human umbilical cord stroma mesenchymal stem cells. *Mol Cell Proteomics*. 2012;11(2):M111.010496. doi:10.1074/mcp.M111.010496
17. McIntyre JA, Jones IA, Danilkovich A, Vangsness CT Jr. The placenta: applications in orthopaedic sports medicine. *Am J Sports Med*. 2018;46(1):234–247. doi:10.1177/0363546517697682
18. Rak Kwon D, Jung S, Jang J, Park GY, Suk Moon Y, Lee SC. A 3-dimensional bioprinted scaffold with human umbilical cord blood-mesenchymal stem cells improves regeneration of chronic full-thickness rotator cuff tear in a rabbit model. *Am J Sports Med*. 2020;48(4):947–958. doi:10.1177/0363546520904022
19. Schwab R, Lim R, Goldberg R. Resolving intestinal fibrosis through regenerative medicine. *Curr Opin Pharmacol*. 2019;49:90–94. doi:10.1016/j.coph.2019.09.011
20. Ibrahim AGE, Li C, Rogers R, et al. Augmenting canonical Wnt signalling in therapeutically inert cells converts them into therapeutically potent exosome factories. *Nat Biomed Eng*. 2019;3 (9):695–705. doi:10.1038/s41551-019-0448-6
21. Gollmann-Tepekoylu C, Polzl L, Graber M, et al. miR-19a-3p containing exosomes improve function of ischemic myocardium upon shock wave therapy. *Cardiovasc Res*. 2020;116(6):1226-1236. doi:10.1093/cvr/cvz209
22. Mori MA, Ludwig RG, Garcia-Martin R, Brandao BB, Kahn CR. Extracellular miRNAs: from biomarkers to mediators of physiology and disease. *Cell Metab*. 2019;30(4):656–673. doi:10.1016/j.cmet.2019.07.011
23. Desmoulière A, Geinoz A, Gabbiani F, Gabbiani G. Transforming growth factor-beta 1 induces alpha-smooth muscle actin expression in granulation tissue myofibroblasts and in quiescent and growing cultured fibroblasts. *J Cell Biol*. 1993;122(1):103–111. doi:10.1083/jcb.122.1.103
24. Wynn TA, Ramalingam TR. Mechanisms of fibrosis: therapeutic translation for fibrotic disease. *Nat Med*. 2012;18(7):1028–1040. doi:10.1038/nm.2807
25. Thum T, Gross C, Fiedler J, et al. MicroRNA-21 contributes to myocardial disease by stimulating MAP kinase signalling in fibroblasts. *Nature*. 2008;456(7224):980–984. doi:10.1038/nature07511
26. Caviglia JM, Yan J, Jang MK, et al. MicroRNA-21 and dicer are dispensable for hepatic stellate cell activation and the development of liver fibrosis. *Hepatology*. 2018;67(6):2414–2429. doi:10.1002/hep.29627
27. Loyer X, Paradis V, Henique C, et al. Liver microRNA-21 is overexpressed in non-alcoholic steatohepatitis and contributes to the disease in experimental models by inhibiting PPARalpha expression. *Gut*. 2016;65(11):1882–1894. doi:10.1136/gutjnl-2014-308883
28. Chau BN, Xin C, Hartner J, et al. MicroRNA-21 promotes fibrosis of the kidney by silencing metabolic pathways. *Sci Transl Med*. 2012;4 (121):121ra118. doi:10.1126/scitranslmed.3003205
29. Cui H, He Y, Chen S, Zhang D, Yu Y, Fan C. Macrophage-derived miRNA-containing exosomes induce peritendinous fibrosis after tendon injury through the miR-21-5p/Smad7 pathway. *Mol Ther Nucleic Acids*. 2019;14:114–130. doi:10.1016/j.omtn.2018.11.006
30. Zhu J, Liu B, Wang Z, et al. Exosomes from nicotine-stimulated macrophages accelerate atherosclerosis through miR-21-3p/PTEN-mediated VSMC migration and proliferation. *Theranostics*. 2019;9 (23):6901–6919. doi:10.7150/thno.37357
31. Théry C, Amigorena S, Raposo G, Clayton A. Isolation and characterization of exosomes from cell culture supernatants and biological fluids. *Curr Protoc Cell Biol*. 2006;30:3–22.
32. Théry C, Witwer KW, Aikawa E, et al. Minimal information for studies of extracellular vesicles 2018 (MISEV2018): a position statement of the international society for extracellular vesicles and update of the MISEV2014 guidelines. *J Extracell Vesicles*. 2018;7(1):1535750.
33. Xiao C, Wang K, Xu Y, et al. Transplanted mesenchymal stem cells reduce autophagic flux in infarcted hearts via the exosomal transfer of miR-125b. *Circ Res*. 2018;123(5):564–578. doi:10.1161/CIRCRESAHA.118.312758
34. de Couto G, Gallet R, Cambier L, et al. Exosomal MicroRNA transfer into macrophages mediates cellular postconditioning. *Circulation*. 2017;136(2):200–214. doi:10.1161/CIRCULATIONAHA.116.024590
35. Yao Z, Wang W, Ning J, et al. Hydroxycamptothecin inhibits peritendinous adhesion via the endoplasmic reticulum stress-dependent apoptosis. *Front Pharmacol*. 2019;10:967. doi:10.3389/fphar.2019.00967
36. Qian Y, Zhao X, Han Q, Chen W, Li H, Yuan W. An integrated multi-layer 3D-fabrication of PDA/RGD coated graphene loaded PCL nanoscaffold for peripheral nerve restoration. *Nat Commun*. 2018;9(1):323. doi:10.1038/s41467-017-02598-7
37. Koob TJ, Summers AP. Tendon–bridging the gap. *Comp Biochem Physiol A Mol Integr Physiol*. 2002;133(4):905–909. doi:10.1016/S1095-6433(02)00255-6
38. Garner WL, McDonald JA, Koo M, Kuhn C 3rd, Weeks PM. Identification of the collagen-producing cells in healing flexor tendons. *Plast Reconstr Surg*. 1989;83(5):875–879. doi:10.1097/00006534-198905000-00018
39. Shi H, Xu X, Zhang B, et al. 3,3′-Diindolylmethane stimulates exosomal Wnt11 autocrine signaling in human umbilical cord mesenchymal stem cells to enhance wound healing. *Theranostics*. 2017;7(6):1674–1688. doi:10.7150/thno.18082

40. Zhu Z, Zhang Y, Zhang Y, et al. Exosomes derived from human umbilical cord mesenchymal stem cells accelerate growth of VK2 vaginal epithelial cells through MicroRNAs in vitro. *Hum Reprod*. 2019;34(2):248–260. doi:10.1093/humrep/dey344
41. Zhang Y, Hao Z, Wang P, et al. Exosomes from human umbilical cord mesenchymal stem cells enhance fracture healing through HIF-1alpha-mediated promotion of angiogenesis in a rat model of stabilized fracture. *Cell Prolif*. 2019;52(2):e12570. doi:10.1111/cpr.12570
42. Sun Y, Shi H, Yin S, et al. Human mesenchymal stem cell derived exosomes alleviate type 2 diabetes mellitus by reversing peripheral insulin resistance and relieving beta-cell destruction. *ACS Nano*. 2018;12(8):7613–7628. doi:10.1021/acsnano.7b07643
43. Ni J, Liu X, Yin Y, Zhang P, Xu YW, Liu Z. Exosomes derived from TIMP2-modified human umbilical cord mesenchymal stem cells enhance the repair effect in rat model with myocardial infarction possibly by the Akt/Sfrp2 Pathway. *Oxid Med Cell Longev*. 2019;2019:1958941. doi:10.1155/2019/1958941
44. Wang H, Wang B, Zhang A, et al. Exosome-mediated miR-29 transfer reduces muscle atrophy and kidney fibrosis in mice. *Mol Ther*. 2019;27(3):571–583. doi:10.1016/j.ymthe.2019.01.008
45. Zhang Q, Lenardo MJ, Baltimore D. 30 years of NF-kappaB: a blossoming of relevance to human pathobiology. *Cell*. 2017;168(1–2):37–57. doi:10.1016/j.cell.2016.12.012
46. Treiber M, Neuhofer P, Anetsberger E, et al. Myeloid, but not pancreatic, RelA/p65 is required for fibrosis in a mouse model of chronic pancreatitis. *Gastroenterology*. 2011;141(4):1473–1485, 1485.e1471-1477. doi:10.1053/j.gastro.2011.06.087
47. Moles A, Sanchez AM, Banks PS, et al. Inhibition of RelA-Ser536 phosphorylation by a competing peptide reduces mouse liver fibrosis without blocking the innate immune response. *Hepatology*. 2013;57(2):817–828. doi:10.1002/hep.26068
48. Zhao QD, Viswanadhapalli S, Williams P, et al. NADPH oxidase 4 induces cardiac fibrosis and hypertrophy through activating Akt/mTOR and NFkappaB signaling pathways. *Circulation*. 2015;131(7):643–655. doi:10.1161/CIRCULATIONAHA.114.011079
49. Wang Q, Jiang H, Li Y, et al. Targeting NF-kB signaling with polymeric hybrid micelles that co-deliver siRNA and dexamethasone for arthritis therapy. *Biomaterials*. 2017;122:10–22. doi:10.1016/j.biomaterials.2017.01.008
50. Xian P, Hei Y, Wang R, et al. Mesenchymal stem cell-derived exosomes as a nanotherapeutic agent for amelioration of inflammation-induced astrocyte alterations in mice. *Theranostics*. 2019;9(20):5956–5975. doi:10.7150/thno.33872
51. Zhang H, Li J, Li G, Wang S. Effects of celastrol on enhancing apoptosis of ovarian cancer cells via the downregulation of microRNA21 and the suppression of the PI3K/AktNFkappaB signaling pathway in an in vitro model of ovarian carcinoma. *Mol Med Rep*. 2016;14(6):5363–5368. doi:10.3892/mmr.2016.5894
52. Kang JY, Park H, Kim H, et al. Human peripheral blood-derived exosomes for microRNA delivery. *Int J Mol Med*. 2019;43(6):2319–2328. doi:10.3892/ijmm.2019.4150
53. Chung KW, Lee EK, Lee MK, Oh GT, Yu BP, Chung HY. Impairment of PPARα and the fatty acid oxidation pathway aggravates renal fibrosis during aging. *J Am Soc Nephrol*. 2018;29(4):1223–1237. doi:10.1681/ASN.2017070802